AIP | Applied Physics Letters

Zinc oxide modified with benzylphosphonic acids as transparent electrodes in regular and inverted organic solar cell structures

Ilja Lange, Sina Reiter, Juliane Kniepert, Fortunato Piersimoni, Michael Pätzel, Jana Hildebrandt, Thomas Brenner, Stefan Hecht, and Dieter Neher

Citation: Applied Physics Letters **106**, 113302 (2015); doi: 10.1063/1.4916182
View online: http://dx.doi.org/10.1063/1.4916182
View Table of Contents: http://scitation.aip.org/content/aip/journal/apl/106/11?ver=pdfcov
Published by the AIP Publishing

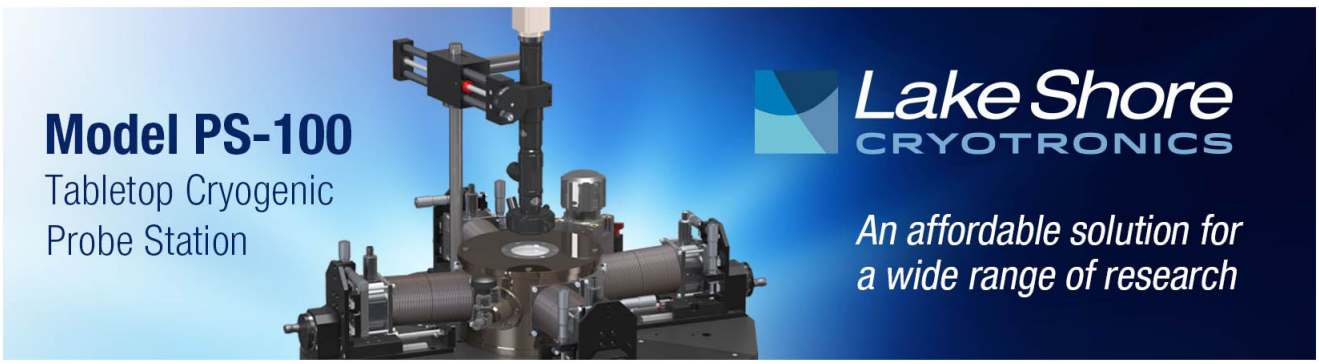

Zinc oxide modified with benzylphosphonic acids as transparent electrodes in regular and inverted organic solar cell structures

Ilja Lange,[1] Sina Reiter,[1] Juliane Kniepert,[1] Fortunato Piersimoni,[1] Michael Pätzel,[2] Jana Hildebrandt,[2] Thomas Brenner,[1] Stefan Hecht,[2] and Dieter Neher[1,a)]
[1]*Institute of Physics and Astronomy, University of Potsdam, Karl-Liebknecht-Strasse 24-25, 14476 Potsdam, Germany*
[2]*Department of Chemistry & IRIS Adlershof, Humboldt-Universität zu Berlin, Brook-Taylor-Str. 2, 12489 Berlin, Germany*

(Received 25 November 2014; accepted 12 March 2015; published online 20 March 2015)

An approach is presented to modify the work function of solution-processed sol-gel derived zinc oxide (ZnO) over an exceptionally wide range of more than 2.3 eV. This approach relies on the formation of dense and homogeneous self-assembled monolayers based on phosphonic acids with different dipole moments. This allows us to apply ZnO as charge selective bottom electrodes in either regular or inverted solar cell structures, using poly(3-hexylthiophene):phenyl-C71-butyric acid methyl ester as the active layer. These devices compete with or even surpass the performance of the reference on indium tin oxide/poly(3,4-ethylenedioxythiophene) polystyrene sulfonate. Our findings highlight the potential of properly modified ZnO as electron or hole extracting electrodes in hybrid optoelectronic devices. © *2015 AIP Publishing LLC*.
[http://dx.doi.org/10.1063/1.4916182]

Transparent metal oxides (TMOs) are integral parts of today's optoelectronic devices, either as electron conducting electrodes or intrinsically doped semiconductors. Among these, zinc oxide (ZnO) is becoming increasingly important, as it is composed of earth-abundant elements. Also, a wide range of vapor and solution based methods are available for ZnO deposition, ranging from chemical or physical vapor deposition (CVD, PVD) for the preparation of epitaxially grown single crystalline ZnO films to sol-gel procedures for low-cost deposition from solution. ZnO is already intensively used as a low-cost, transparent electrode in inorganic devices,[1,2] but more recently also as a charge selective interlayer material in efficient organic solar cells (OSCs) or organic light-emitting diodes (OLEDs).[3,4] However, the moderate work function (WF) of untreated ZnO of about 4.3 eV causes injection barriers to almost all conventional organic semiconductors[5–9] and the WF of such ZnO layers is poorly reproducible due to the physisorption of contaminations.[10] On the other hand, its poor chemical stability in an acidic environment[11–13] makes the modification of the ZnO WF particularly challenging. For some of the recent organic record solar cells, the WF of the ZnO forming the bottom electrode was lowered by applying an electrolytic (ionic) buffer layer such as polyethyleneimine (PEI) or ethoxylated polyethyleneimine (PEIE).[14] However, the chemical and physical structure of the ZnO/PEI/OSC interface is still not understood.

An elegant way to alter the WF and, at the same time, passivate the ZnO surface is the attachment of a self-assembled monolayer (SAM) of polar molecules. SAM modifications have already been applied to other transparent metal oxides such as indium tin oxide (ITO);[15–17] however, deposition of these mostly acidic molecules onto ZnO is well-known to cause etching of the chemically less stable ZnO surface.[18,19] Therefore, recent attempts drastically reduced the exposure time to the acidic environment simply by spin coating the solution of the SAM forming molecules onto ZnO.[20,21] However, given the short time for molecular assembly, the quality of the so-formed monolayer might be ill defined. Indeed, SAM formation via spin coating yielded a rather small shift of the WF, indicating a sparse coverage.

Recently, we related the degree of etching of the ZnO surface upon SAM preparation to the water content in the molecular solution (and therefore a reduced protonation of the phosphonic acid (PA) molecules).[5] Experiments on well-defined single crystalline ZnO (0001) and (000–1) surfaces proved that etching during immersion can be fully suppressed if dried ethanol (<0.01% H_2O) is used as the solvent. A preparation protocol was developed which results in a very dense and homogenous molecular monolayer of oriented molecules on ZnO substrates. The resulting SAMs were characterized by a range of complementary techniques, revealing the coverage of the ZnO surface by a dense monolayer with a tilting angle α of the aromatic ring with respect to the ZnO surface of $47° \pm 3°$, which is in perfect agreement to the previous theoretical predictions on that system for tridental binding of the phosphonic acid anchoring group to the substrate.[22] By employing substituted benzyl PAs (BPA) as well as pyrimidine PA (PyPA) with different dipole moments of the head group, we altered the WF (measured with Kelvin Probe (KP) inside a glovebox) of these singly crystalline ZnO substrates from about 4.1 eV to almost 5.7 eV. A strict linear relation between the dipole moment and the resulting WF was thereby observed, which is in agreement with the prediction of the Helmholtz equation. From the analysis of this linear relation, a molecular density of $\sim 2\,nm^{-2}$ was concluded, which is close to the theoretical maximum of

a)Author to whom correspondence should be addressed. Electronic mail: neher@uni-potsdam.de

$2.73\,nm^{-2}$.[22] Atomic force microscopy (AFM) and scanning Kelvin probe microscopy (SKPM) revealed a very homogenous SAM structure at least at the few 10 nm scale. The wide achievable WF range allowed us already to apply the modified ZnO as highly selective electron-injecting as well as hole-injecting contact in electron- or hole-only diodes, simply by varying the used SAM molecule, proving the electronic grade of the so prepared ZnO/SAM electrodes.

Here, we extend these investigations to the commercially more relevant, though structurally less defined, polycrystalline surface of sol-gel processed ZnO. We are able to tune the WF of this sol-gel processed ZnO over an exceptionally wide range of more than 2.3 eV, enabling the application as efficient transparent cathode in inverted poly(3-hexylthiophene):phenyl-C71-butyric acid methyl ester (P3HT:PCBM) solar cell structures and also as efficient anode in regular structures. Thereby, the best devices with SAM-modified ZnO electrodes compete with or even exceed the performance of the regular benchmark system comprising an ITO/poly(3,4-ethylenedioxythiophene) polystyrene sulfonate (PEDOT:PSS) electrode, highlighting again the potential of the method.

As ZnO substrates either (10–10) single crystals (CrysTec GmbH, Germany) or sol-gel processed ZnO was used. The sol-gel ZnO films were prepared according to the literature[4] via spin coating the solution of 100 mg zinc acetate dihydrate in 1 ml 2-methoxyethanol with 27.7 μl ethanolamine onto ITO-covered glass, yielding a ~30 nm thick layer followed by subsequent annealing at 200 °C for 1 h to promote crystallization. PA molecules for SAM formation (for chemical names and supplier see Ref. 5) were dissolved in dried ethanol (SeccoSolv®, Merck Millipore, <0.01% H_2O) at a concentration of 2 mM inside a glovebox to prevent water adsorption. Preparation of the SAMs was performed by immersing the ZnO substrates into this solution on a hot plate at 70 °C in covered glass vessels, subsequent gentle purging in ethanol and drying at 90 °C for 3 min on a hot plate. For solar cells, P3HT:PC_{71}BM (Rieke Metals, Inc./Solenne) bulk heterojunction layers in a 1:1 (wt./wt.) ratio were prepared by spin coating from a chloroform solution and annealed at 150 °C for 15 min on a hot plate. 10 nm Sm/100 nm Al (regular) or 7 nm MoO_3/100 nm Ag (inverted) top electrodes were evaporated on top leading to pixel sizes of $6\,mm^2$.

The three most stable facets of a ZnO crystal are the two polar (0001)-Zn and (000–1)-O as well as the mixed terminated (10–10) surface.[23] It can be expected that also the surface of such sol-gel processed ZnO layers consists mainly of these three facets. We, therefore, first tested our approach to the mixed terminated (10–10) single crystalline surface. Again, annealing the single crystal samples at 1180 °C for 6 h precipitated a well-defined smooth terraced surface (see Figure 1(a)). Following the protocol described in Ref. 5, SAMs from various BPAs and PyPA (see Figure 2(a)) were prepared on top of these ZnO substrates. We again find that the WF shift is largest for a specific optimum of immersion time, between 20 min and 2 h. Smaller WF shifts for non-optimized immersion are supposedly due to an incomplete coverage for shorter times or stable multilayer formation at longer times. The absolute WF as function of the molecular head-group dipole moment of the mixed terminated ZnO surface (Figure 2(b)) agrees thereby nicely with the results obtained on the two modified polar surfaces, resulting in equal slopes in that diagram. Kedem *et al.* recently noted that the particular choice of the ZnO substrate has only little effect on the resulting WF upon phenylphosphonate treatment.[24] Although the (10–10) ZnO surface differs geometrically from the two polar surfaces and supports a rather

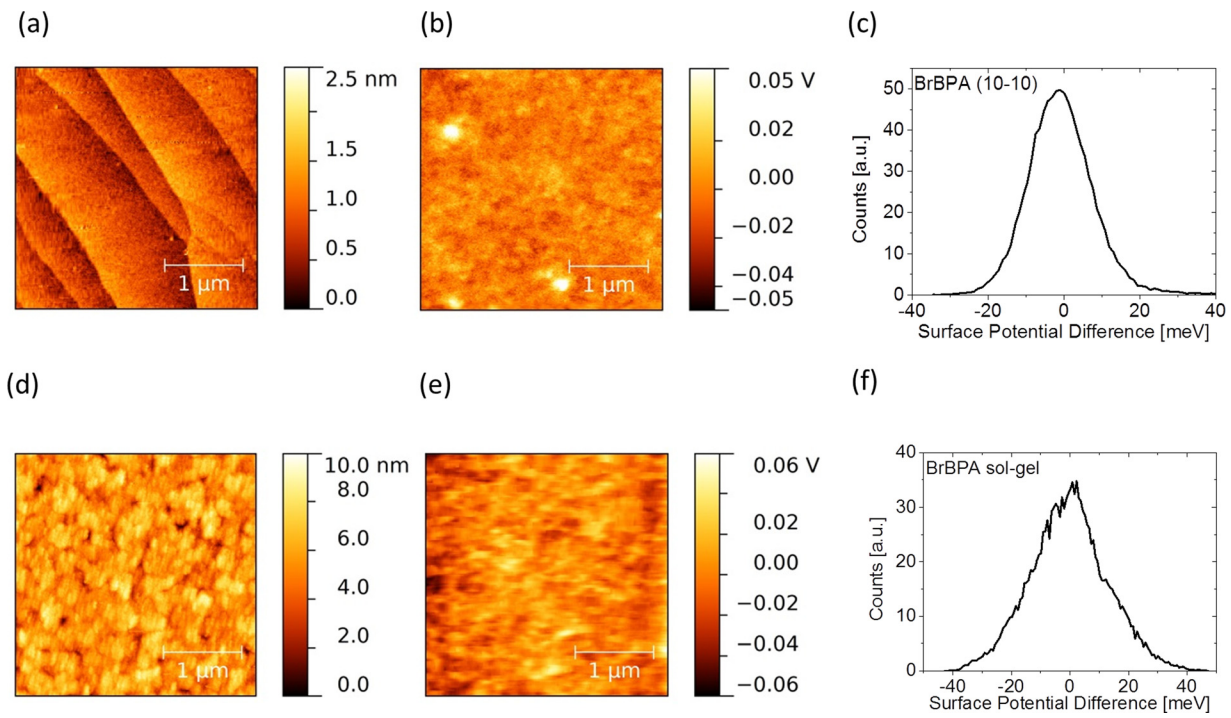

FIG. 1. AFM (a) and (d), SKPM (b) and (e), and SKPM histograms (c) and (f) of BrBPA-SAM covered single crystalline (10-10) (a)–(c) or polycrystalline sol-gel processed (d)–(f) ZnO substrates.

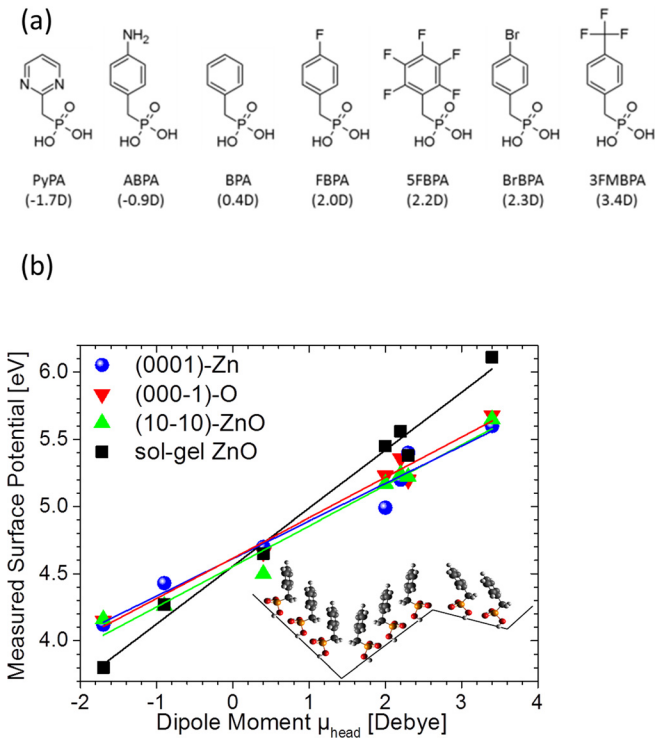

FIG. 2. (a) Chemical structures of the applied SAM-forming phosphonic acids with their respective molecular dipole moment of the head group in brackets. (b) Measured surface potential (KP) as function of the molecular head group dipole moment of the three single crystalline and the sol-gel processed ZnO surfaces covered with the molecular SAMs displayed above. The strict linear relation agrees with the Helmholtz equation. The slightly larger slope of the sol-gel processed ZnO is most likely caused by a preferential upright orientation of the molecular head group on the rougher surface structure (inset).

bidentate binding of the PA, we conclude that the effects on surface coverage and molecular tilt are negligible. Furthermore, our AFM and SKPM measurements revealed also on the (10–10) ZnO surface a very homogenous coverage with a small variation of the local WF and without etching effects (Figures 1(a)–1(c)). We can therefore conclude that a similarly high SAM quality is obtained on the mixed terminated (10–10) ZnO surface, notably with the same preparation parameters as used for the two polar surfaces.

Having established a preparation protocol for PA-based SAMs on the three important ZnO crystal surfaces, we then turned to modifying the polycrystalline surface of sol-gel prepared ZnO. Notably, to reach a maximum WF shift of the sol-gel ZnO, immersion times between 20 min and 2 h were needed which is equivalent to what was used for the single crystalline surfaces, albeit with no significant further change for even longer immersion times. However, for ideal electronic behavior, it turned out that the immersion time needed to be increased to about 4 h, presumably due to a filling/passivation of holes in the porous ZnO layer. The resulting WFs as a function of the dipole moment of the SAM molecules head group are also shown in Figure 2. Notably, comparable or even stronger WF shifts were observed on these polycrystalline sol-gel prepared substrates, covering an exceptionally wide WF range from 3.8 eV to above 6.1 eV.

According to the Helmholtz equation, the WF shift is proportional to the dipole moment component perpendicular to the surface $\mu_\perp = \mu \times \sin\alpha$ and to the number of dipoles per area N/A

$$\Delta WF = \frac{e \times \mu \times \sin\alpha}{\varepsilon_0 \times k_{red}} \times \frac{N}{A}, \quad (1)$$

where e denotes the elementary charge and ε_0 is the vacuum permittivity. k_{red} accounts for the depolarization of the molecules in close proximity and is about 2 in this system.[25] A plausible explanation for the higher WF shifts arises from the fact that the sol-gel prepared ZnO has a significantly larger surface roughness compared to the terraced, well-defined single crystalline surface (see Figure 1). Such a larger surface roughness causes a larger effective surface area, supporting more binding sites for the PAs; however, a tilt of the local surface reduces also $\mu_\perp$ in the same quantity. We propose instead a non-isotropic distribution of the molecular tilt resulting in a more upright orientation of the head group with respect to the surface plane on this particular rough surface (see inset in Fig. 2(b)). Given the comparable WF shifts when modifying the three stable surfaces of ZnO (Fig. 2(b)), we expect that possible differences in bond dipoles or surface reorganization of the different ZnO substrates are quite similar, and that they do not account for the different WF(μ_{head}) slope of the modified sol-gel processed ZnO. Interestingly, the SKPM measurements in Figure 1 reveal an only minor increase of the lateral WF variations after SAM-modification compared to the single-crystalline ZnO surface. We therefore conclude that a well-defined, high quality SAM is also formed on the sol-gel ZnO.

With the WF being tunable over a wide range, these modified sol-gel processed ZnO films can be applied as an efficient transparent cathode in inverted solar cells, but also as the transparent anode in regular P3HT:PCBM solar cell structures without the need of additional buffer layers such as PEDOT:PSS. For the inverted structure, the sol-gel ZnO surface was modified by an aminobenzyl PA (ABPA) SAM, yielding a WF of about 4.25 eV. Alternatively, trifluoromethylbenzyl PA (3FMBPA) was used to prepare a ZnO-based anode with a WF of about 6.1 eV for regular cells. A benchmark reference cell on ITO/PEDOT:PSS in a regular structure was also prepared for comparison.

The resulting J-V-curves under illumination are shown in Figure 3 with the respective performance parameters of the best performing devices in Table I. At least 10 pixels of each type were measured and device performance deviated around 10%. The solar cells comprising ZnO as bottom electrode show an exceptionally good performance, with a power conversion efficiency (PCE) of the inverted structure distinctly exceeding the reference value of the benchmark cell on ITO/PEDOT:PSS. Notably, also the regular solar cell comprising the 3FMBPA-SAM modified ZnO as the anode displays a high PCE and fill factor (FF), comparable to that of the ITO/PEDOT:PSS reference cell, highlighting again the electronic grade of our SAM-modified ZnO electrodes. As a general trend, all ZnO-based devices benefit from a higher short circuit current (J_{SC}); however, this effect is most distinct in the inverted structure with an almost 20% higher J_{SC} with respect to the reference cell. The origin of such an increase was recently attributed to a more ideal optical field

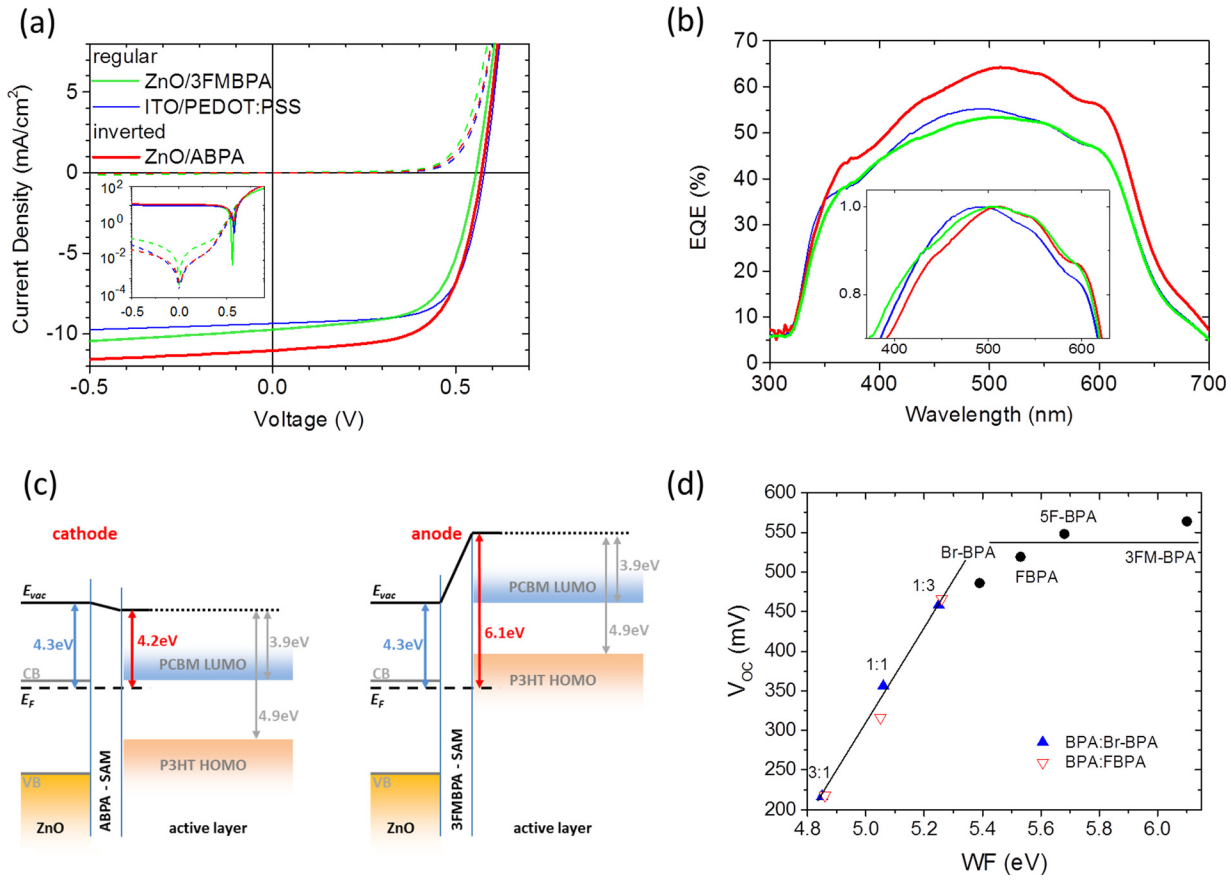

FIG. 3. (a) *J-V*-curves of all investigated P3HT:PCBM solar cells with different electrodes and architectures under illumination (full line) and in the dark (dashed line). Inset: semi-logarithmic *J-V* plot. (b) EQE spectra of the respective devices with the normalized spectra displayed in the inset. (c) Energy level diagram of the contact between the SAM-modified ZnO used as cathode (left) or anode (right) and the P3HT:PCBM blend. (d) V_{oc} of P3HT:PCBM solar cells with differently modified ZnO bottom layers and Sm/Al top electrodes The lines are solely a guide to the eye.

profile in inverted solar cells.[26] Other possible effects will be addressed below. Interestingly, replacing PEDOT:PSS with the 3FMBPA-modified ZnO has an only weak effect on the overall photovoltaic characteristics, though the modified ZnO is not expected to serve as an electron-blocking layer. Recent work pointed out that blocking of minority carriers is important in order to suppress surface recombination.[27] On the other hand, experimental and simulation work by Würfel and coworkers on P3HT:PCBM based solar cells with different cathode and anode materials revealed a strong correlation between the electrode work function (relative to the majority carrier transport level) and the degree of surface recombination.[28] For ohmic contacts, surface recombination was largely suppressed. This is due to the fact that diffusion of majority charges from the electrode into the organic semiconductor results in the formation of a space charge layer near the electrode, accompanied by significant band bending,[29] which prevents minority carriers to reach the contact. In agreement with this finding, recent device simulations of P3HT:PCBM sandwiched between PEDOT:PSS and Sm/Al revealed a negligible effect of surface recombination on the *J-V*-characteristics of P3HT:PCBM devices.[30] Surface recombination will, however, become important for poorly injecting contacts, resulting in a significant decrease of V_{oc}.[28] Indeed, we observe a strong drop of V_{oc} when reducing the WF of the ZnO bottom electrode (Fig. 3(d)). The data reveal that properly modified ZnO is indeed suited to achieve a high V_{oc}, but that the ZnO WF must be significantly larger than the P3HT:PCBM ionization potential to realize conditions comparable to the regular device with the PEDOT:PSS anode, the latter having good electron blocking properties.

TABLE I. Device parameters of the best performing solar cells. At least 10 cells of each type were measured and device performance deviated around 10%.

Bottom electrode	PCE (%)	V_{OC} (V)	J_{SC} (mA/cm^2)	*FF* (%)
Regular				
ZnO/3FMBPA SAM	3.82	0.560	9.8	63.4
ITO/PEDOT:PSS	3.97	0.578	9.3	67.9
Inverted				
ZnO/ABPA SAM	4.22	0.570	11.0	63.3

The overall increase of J_{SC} in regular or inverted solar cells prepared on ZnO electrodes goes along with corresponding changes in the EQE spectra as shown in Figure 3(b). One reason for this improvement might be the higher transparency of ZnO, allowing more light to reach the active layer. However, the normalized external quantum efficiency (EQE) spectra shown in the inset of Figure 3(b) also reveal a more pronounced shoulder at 550 nm and 600 nm, which points to a more crystalline P3HT phase in the blends coated on ZnO. This finding is, in turn, consistent with the lower

V_{OC} measured on some of the ZnO-based devices, as a higher degree of crystallinity of the polymer in P3HT:PCBM blends is known to reduce the effective band gap between the donor HOMO and acceptor LUMO.[31]

In conclusion, we have modified the WF of solution-processed sol-gel derived ZnO by employing BPA-based SAMs with different dipole moments. For this purpose, a recently developed protocol for the formation of SAMs on highly defined single-crystalline ZnO was adopted to the less defined surfaces of sol-gel processed ZnO.[5] This modification caused the WF to vary over an exceptionally large range spanning more than 2.3 eV, which enabled us to apply ZnO as hole injecting/extraction interlayer in regular solar cell structures. Efficiency measurements of regular and inverted P3HT:PCBM solar cells showed that these fully solution processed interlayers lead to a competitive or even increased device performance, compared to the reference cells on ITO/PEDOT:PSS. As these SAM-modified ZnO layers can be coated via solution-based methods on virtually any electrode material, the presented approach paves the way to ITO-free devices without the need for including electrolyte buffer layers. The tunability from cathode to anode by our approach opens additional freedom in device design and emphasizes the importance of understanding the role of the WF on injection and extraction of charges.

This work was financially supported by the Deutsche Forschungsgemeinschaft (DFG) within the Collaborative Research Centre HIOS (SFB 951) and the SPP 1355. T.B. was supported by the Helmholtz Energy Alliance for Hybrid Photovoltaics.

[1]K. Ellmer, A. Klein, and B. Rech, *Transparent Conductive Zinc Oxide: Basics and Applications in Thin Film Solar Cells* (Springer, Berlin, 2008).
[2]H. Liu, V. Avrutin, N. Izyumskaya, Ü. Özgür, and H. Morkoç, Superlattices Microstruct. **48**, 458 (2010).
[3]D. Kabra, L. P. Lu, M. H. Song, H. J. Snaith, and R. H. Friend, Adv. Mater. **22**, 3194 (2010).
[4]Y. Sun, J. H. Seo, C. J. Takacs, J. Seifter, and A. J. Heeger, Adv. Mater. **23**, 1679 (2011).
[5]I. Lange, S. Reiter, M. Pätzel, A. Zykov, A. Nefedov, J. Hildebrandt, S. Hecht, S. Kowarik, C. Wöll, G. Heimel, and D. Neher, Adv. Funct. Mater. **24**, 7014 (2014).
[6]V. Bhosle, J. T. Prater, F. Yang, D. Burk, S. R. Forrest, and J. Narayan, J. Appl. Phys. **102**, 023501 (2007).
[7]Y. H. Kim, J. S. Kim, W. M. Kim, T.-Y. Seong, J. Lee, L. Müller-Meskamp, and K. Leo, Adv. Funct. Mater. **23**, 3645 (2013).
[8]J. C. Bernède, L. Cattin, M. Morsli, and Y. Berredjem, Sol. Energy Mater. Sol. Cells **92**, 1508 (2008).
[9]K. N. Pradipta, Y. Jihoon, K. Jinwoo, C. Seungjun, J. Jaewook, L. Changhee, and H. Yongtaek, J. Phys. D: Appl. Phys. **42**, 035102 (2009).
[10]C. Wöll, Prog. Surf. Sci. **82**, 55 (2007).
[11]T. Minami, Semicond. Sci. Technol. **20**, S35 (2005).
[12]M. Jørgensen, K. Norrman, and F. C. Krebs, Sol. Energy Mater. Sol. Cells **92**, 686 (2008).
[13]J.-H. Park, S. J. Kang, S.-I. Na, H. H. Lee, S.-W. Kim, H. Hosono, and H.-K. Kim, Sol. Energy Mater. Sol. Cells **95**, 2178 (2011).
[14]Y. Zhou, C. Fuentes-Hernandez, J. Shim, J. Meyer, A. J. Giordano, H. Li, P. Winget, T. Papadopoulos, H. Cheun, J. Kim, M. Fenoll, A. Dindar, W. Haske, E. Najafabadi, T. M. Khan, H. Sojoudi, S. Barlow, S. Graham, J.-L. Brédas, S. R. Marder, A. Kahn, and B. Kippelen, Science **336**, 327 (2012).
[15]P. J. Hotchkiss, H. Li, P. B. Paramonov, S. A. Paniagua, S. C. Jones, N. R. Armstrong, J.-L. Brédas, and S. R. Marder, Adv. Mater. **21**, 4496 (2009).
[16]A. Sharma, A. Haldi, P. J. Hotchkiss, S. R. Marder, and B. Kippelen, J. Appl. Phys. **105**, 074511 (2009).
[17]B. A. MacLeod, N. E. Horwitz, E. L. Ratcliff, J. L. Jenkins, N. R. Armstrong, A. J. Giordano, P. J. Hotchkiss, S. R. Marder, C. T. Campbell, and D. S. Ginger, J. Phys. Chem. Lett. **3**, 1202 (2012).
[18]A. Bulusu, S. A. Paniagua, B. A. MacLeod, A. K. Sigdel, J. J. Berry, D. C. Olson, S. R. Marder, and S. Graham, Langmuir **29**, 3935 (2013).
[19]O. Taratula, E. Galoppini, D. Wang, D. Chu, Z. Zhang, H. Chen, G. Saraf, and Y. Lu, J. Phys. Chem. B **110**, 6506 (2006).
[20]Y. E. Ha, M. Y. Jo, J. Park, Y.-C. Kang, S. I. Yoo, and J. H. Kim, J. Phys. Chem. C **117**, 2646 (2013).
[21]S. R. Cowan, P. Schulz, A. J. Giordano, A. Garcia, B. A. MacLeod, S. R. Marder, A. Kahn, D. S. Ginley, E. L. Ratcliff, and D. C. Olson, Adv. Funct. Mater. **24**, 4671 (2014).
[22]C. Wood, H. Li, P. Winget, and J.-L. Brédas, J. Phys. Chem. C **116**, 19125 (2012).
[23]O. Dulub, L. A. Boatner, and U. Diebold, Surf. Sci. **519**, 201 (2002).
[24]N. Kedem, S. Blumstengel, F. Henneberger, H. Cohen, G. Hodes, and D. Cahen, Phys. Chem. Chem. Phys. **16**, 8310 (2014).
[25]G. Heimel, L. Romaner, E. Zojer, and J.-L. Brédas, Nano Lett. **7**, 932 (2007).
[26]S. Albrecht, S. Schäfer, I. Lange, S. Yilmaz, I. Dumsch, S. Allard, U. Scherf, A. Hertwig, and D. Neher, Org. Electron. **13**, 615 (2012).
[27]E. L. Ratcliff, A. Garcia, S. A. Paniagua, S. R. Cowan, A. J. Giordano, D. S. Ginley, S. R. Marder, J. J. Berry, and D. C. Olson, Adv. Energy Mater. **3**, 647 (2013).
[28]J. Reinhardt, M. Grein, C. Bühler, M. Schubert, and U. Würfel, Adv. Energy Mater. **4**, 1400081 (2014).
[29]I. Lange, J. C. Blakesley, J. Frisch, A. Vollmer, N. Koch, and D. Neher, Phys. Rev. Lett. **106**, 216402 (2011).
[30]J. Kniepert, I. Lange, N. J. van der Kaap, L. J. A. Koster, and D. Neher, Adv. Energy Mater. **4**, 1301401 (2014).
[31]I. Lange, J. Kniepert, P. Pingel, I. Dumsch, S. Allard, S. Janietz, U. Scherf, and D. Neher, J. Phys. Chem. Lett. **4**, 3865 (2013).